

“Evaluation Of high resolution Ultrasound With color Doppler findings In Malignant Cervical Lymphadenopathy”

Dr. Disha Mittal*, Dr. Sanjay Dhawan**,

*Department of Radiodiagnosis, Assistant Professor (PGIMS Rohtak) India.

**Department of Radiodiagnosis, Paras Hospital, Gurugram, Haryana, India.

Corresponding Author: Dr. Disha Mittal

Abstract: Objective: This study aimed to assess the findings of high resolution ultrasound with color Doppler in detecting malignant cervical lymphadenopathy and correlation with cytology and the efficacy of high resolution ultrasound in detecting malignant cervical lymphadenopathy.

Materials and Methods: We evaluated 93 cases of malignant cervical lymphadenopathy, referred for USG and color doppler evaluation of the neck. All of USG and color doppler findings were correlated with cytopathological / histopathological findings.

Results: In our study, 58 % (54/93) of malignant nodes were unilateral. Short axis >10 mm was seen in 92% of malignant lymph nodes. In our study 68% malignant nodes were round on USG. Blurring of margins was seen in 32% of malignant nodes on USG. Hilum was absent in 71% of malignant lymph nodes on USG. In our study 45% of malignant lymph node were hypoechoic on USG. Necrosis was seen in 67.7% of malignant lymph nodes on USG. Matting was found in 42% cases of malignant nodes. Calcification was seen in 3 malignant cervical lymph nodes. Malignant nodes showed predominantly mixed and hilar vascularity on color Doppler. lymph nodes showed the RI cut-off value -0.77 and PI cut-off value -1.61 in differentiating benign and malignant nodes.

Conclusion: Gray scale USG coupled with Doppler is a useful investigation in the evaluation of malignant cervical adenopathy and is complementary to the CECT as it is non-invasive, inexpensive, readily available and free of radiation.

Keywords: Cervical lymphadenopathy, Ultrasound, color Doppler, Malignant nodes.

Date of Submission: 17-05-2019

Date of acceptance: 02-06-2019

I. Introduction

Cervical lymph nodes are common sites of metastases from head and neck cancer, and in lymphoma (1). Ultrasound is a useful imaging tool in evaluation of cervical lymph nodes. Gray scale along with color and power Doppler sonography are commonly used in clinical practice. The sonographic appearances of normal nodes differ from those of abnormal nodes. Sonographic features to characterize abnormal nodes are shape, size, hilum, echogenicity, calcification, intranodal necrosis (1,2,3). Color Doppler ultrasound (CDUS) define the morphologic and vascular characteristics of enlarged lymph nodes (4,5). The presence of intranodal vascularity, its distribution, estimation of the intravascular resistance and spectral doppler analysis are evaluated with color Doppler (6).

Cervical nodal metastases have a major influence on the prognosis of patients with head and neck tumors. These metastases influence not only the risk of local recurrence, but also the risk of distant metastases (7,8,9,10).

II. Aims And Objectives

The Aims of this study were to evaluate the ultrasound, Color Doppler findings in enlarged malignant cervical lymph nodes with histopathological / cytopathological correlation and to evaluate the efficacy of high resolution ultrasound in detecting malignant cervical lymphadenopathy.

III. Materials And Methods

The study was conducted during the period from May, 2011 to Jan, 2015. All the cases suspected of having cervical lymphadenopathy or patient with suspected or known primary in the neck referred for USG evaluation of the neck were included in the study. Cases for which cytopathological/histopathological correlation could not be obtained, were excluded from the study.

USG Protocol

USG was performed on Siemens Sonoline Antares Machine with high frequency linear transducers VFX 10-5 MHz and VFX 13-5 MHz. In all cases, representative superficial lymph node was evaluated with respect to size, shape, echo texture and color Doppler findings. Data was analyzed using software SPSS version 15 statistical analysis software. On USG lymph nodes were assessed for Distribution, Anatomical site [According to imaging based nodal classification (adopted from Som P.M. Curtin H.D. Mancuso A.A.) (Table 1)(11)] Size, Shape, Outline, Hilum, Echogenicity, Calcification, Intranodal necrosis, Matting, Color Doppler study -a) Vascular pattern [Hilar, Avascular, Peripheral, Mixed (Fig. 1)] b) Doppler indices [Resistive Index (RI) Pulsatility Index (PI)].

Statistical Analysis

Data was analyzed using software SPSS version 15 statistical analysis software. The values were represented in number (percent) and Mean \pm SD. Chi square test, ANOVA, Fisher exact test and unpaired student's t-test were used. Receiver operating characteristic (ROC) curve is used to find optimal cut-off point for RI and PI to classify benign Vs malignant. p-value less than 0.05 was considered as significant. All of USG and Doppler findings were correlated with cytopathological / histopathological findings.

IV. Results

Total 150 cases of cervical lymphadenopathy were evaluated in the study. According to final cytopathological/histopathological diagnosis, 93 were malignant, out of which 66(44%) were metastatic while 27 (18%) were lymphomatous nodes.

The mean age of metastatic subjects was 57.09 \pm 7.93 years whereas that of subjects with lymphoma was 41.233 \pm 22.93 years.

Among malignant cases, the proportion of males was significantly higher as compared to females which was statistically significant (p<0.001).

Neck swelling was the commonest complaint in all cases of cervical lymphadenopathy.

Morphology Of Malignant Cervical Lymphadenopathy On Gray Scale USG (Table:2)

In our study, 58 % (54/93) of malignant nodes were unilateral 68.2% (45/66) of metastatic nodes, while 44.4% (12/27) of lymphomatous nodes were unilateral and majority of benign nodes were unilateral 57.9% (33/57).

In our study, Short axis >10 mm was seen in 92% of malignant lymph nodes (68.2% metastatic lymph nodes and 88.9% of lymphomatous nodes).

In this study 68.2% (45/66) of metastatic lymph nodes and 66.7% (18/27) of lymphomatous nodes were round in shape.

Blurring of margins, suspicious of extranodal extension was seen in 32% of malignant nodes on USG [36.4 % (24/66) cases of metastatic lymph nodes and 22.2% (2/27) of lymphomatous nodes].

Hilum was absent in 72.7% (48/66) of metastatic lymph node and 66.7% (18/27) of lymphomatous nodes.

In our study 42(63.6%) of metastatic lymph nodes were heteroechoic while 18(66.7%) cases of lymphomatous nodes were hypoechoic.

In this study 77.3% (51/66) of metastatic lymph nodes and 44.4% (12/27) of lymphomatous nodes had necrosis. Necrosis was more in metastatic group as compared to lymphoma group (p=0.037) (Figs. 2,3). Intranodal calcification was seen in 9 cases in our study (Fig. 4).

Matting was found in 50 % (33/66) cases of metastatic lymph nodes and 22.2% (6/27) of lymphomatous nodes in this study.

Comparison of USG findings did not reveal a statistically significant difference for any of the findings except echotexture and necrosis. As compared to lymphomatous group, the proportion of patients with metastatic disease show more heterogeneous echotexture (p=0.042).

Doppler Examination Findings In Malignant Cervical Lymphadenopathy (Table: 3)

Metastatic lymph nodes showed peripheral vascularity in 36.4% (24/66), hilar vascularity in 31.81% (21/66) and mixed in 31.8% (21/66) cases. While 44.4% (12/27) cases of lymphomatous nodes showed mixed pattern of vascularity. As regards vascularity findings, no significant intergroup difference was observed (p>0.05).

For RI, the cut-off value 0.77 was observed i.e. 74.2% sensitive and 78.9% specific whereas for PI, the cut-off value 1.61 was observed representing 74.2% sensitivity and 68.4% specificity in differentiating benign and malignant nodes.

The sensitivity of RI for differentiating between pathologies ranged from 72.7% to 85.7% whereas the specificity ranged from 63.2% to 71.4%. The sensitivity of PI ranged from 71.4% to 91.7% while specificity ranged from 51.2% to 78.9%. (Table 3).

On the basis of USG with color Doppler, out of 150 cases 78 were detected to be malignant and 72 were detected to be benign. However, there were 24 false negative malignant and 9 false positive benign nodes. Overall the sensitivity of USG was 74.2% and specificity was 88.5%. The positive predictive value for malignancy was 88.5% while negative predictive value was 66.7%. Overall diagnostic accuracy was 78%.

V. Discussion

Lymphadenopathy was more common in the level II suggesting that it is the most commonly involved nodal chain.

Level IB nodes cannot be adequately evaluated by ultrasound. USG is not a good modality to differentiate between level II and level III because of mobility of cricoid cartilage during examination.

In patients with a known primary tumour, the distribution of metastatic nodes helps to identify metastases and assists tumour staging. However, if the primary tumour is not identified, the distribution of proven metastatic nodes may give a clue to identify the primary. Specific distribution is also found in lymphomatous and tubercular nodes(1,7,12)(Table 4).

Oral cavity tumors, nasopharyngeal carcinoma, epiglottic and midline tumors, frequently drain bilaterally (7).

The level I and II lymph nodes are often the first to be involved in oral cavity squamous cell carcinoma (13). Level II, III, IV nodes together are major drainage regions from carcinoma of nasopharynx, oropharynx, hypopharynx and larynx(14). However, evaluation of level IB nodes by ultrasound is fraught with difficulties, and the low sensitivity may be due to some of the nodes being situated in the submandibular niche and thus getting hidden by the body of mandible, these nodes cannot be adequately evaluated by ultrasound.

The distribution of nodal size was not significantly different for benign and malignant nodes neither any difference was observed between primary and secondary nodal malignancies (15). Therefore, it has been concluded that lymph node size is not a reliable parameter for the evaluation of metastatic involvement(7).

L/T ratio was greater than 2 in 14% of lymphomatous nodes and smaller than 2 in 85% of metastatic lymph nodes (16).

Ratio of longitudinal and transverse diameters >2 indicated inflammatory disease in 84% cases whereas <1.5 favored metastatic involvement in 71% of cases (17). In our study shape was not statistically significant in determining malignant lymph nodes.

Extranodal spread is radiologically characterized by ablation of fat planes and irregular nodal border. The extracapsular nodal spread or extension of metastatic tumor beyond the lymph node capsule is diagnosed when there is presence of poorly defined margins of the node. These criteria are accurate, only if the patient has not recently had surgery, irradiation, an active infection or inflammation in the area (7,18).

Extracapsular spread is a poor prognostic indicator and associated with reduced survival (7). One previous study reported extra-capsular invasion in 41% of metastatic nodes which was similar to our study (19).

Nodal metastases can invade adjacent muscle, bone, neural, and vascular structures. Loss of fascial planes is the most sensitive sign of arterial invasion, and narrowing or irregularity of the artery is the most specific sign of arterial invasion (17).

The hilum is a good sign of a normal or reactive node and is identified in 90% of normal nodes >5 mm in size by USG (20), but is identified inconsistently by MRI and CT. The hilum was absent in over 90% of metastatic nodes (16).

Absence of hilum was seen in 57-91% of malignant lymph nodes (20). It has been reported that less than 5% of metastatic nodes have a hyperechoic hilum(21). On the other hand, some authors have reported that hyperechoic hilum was visualized in up to 51.5% of metastatic nodes(15).

Metastatic nodes are usually hypoechoic, except for metastases from papillary carcinoma of the thyroid which tend to be hyperechoic (1,5).

Papillary carcinoma of the thyroid show intranodal calcification, and the calcification is usually fine or punctate, peripherally located and may show fine threads of acoustic shadowing (1,22). It is documented in previous study that Hodgkin's lymphoma nodes treated with irradiation or chemotherapy may calcify (23,24). Calcification was also reported in untreated Hodgkin's lymphoma and non Hodgkin's lymphoma (25,26).

Lymph nodes with intranodal necrosis are considered to be pathologic. Intranodal necrosis can be classified into coagulative necrosis and cystic necrosis in which cystic necrosis is more common than coagulative necrosis (1). Coagulative necrosis which appears as an echogenic focus may be found in metastatic nodes. Cystic necrosis is common in metastatic nodes from squamous cell carcinomas and papillary carcinoma of the thyroid (1,4,7).

Analysis of detection of necrosis in the malignant lymph nodes showed an accuracy, sensitivity and Specificity 77%, and 93% for USG(27).

Lymphomatous nodes seldom show cystic necrosis unless the patient has previous radiation therapy or chemotherapy, or has advanced disease (1,7).

Most of the gray scale USG findings were not statistically significant still can help in differential diagnosis of cervical lymphadenopathy. However, because of some overlapping in sonographic appearances of benign and malignant nodes, this modality may not have definite diagnostic values.

For differentiation between various causes of lymphadenopathy most significant factor were echotexture and necrosis on USG. Different patterns of vascularity were predominantly observed viz. mixed, hilar in lymphomatous nodes and peripheral in metastatic nodes.

On PD-US, the hilar pattern was more frequently associated with benignancy (91%) and the peripheral, miscellaneous vascular pattern with malignancy (91%). Benign and malignant lymph nodes showed avascular pattern in 58% and 42% cases respectively(28).

In one previous study metastatic nodes showed a combination of peripheral and central vascularity while in our study, peripheral, mixed and hilar types of vascularity were noted in metastatic nodes (29).

The finding in our study was comparable with a previous study which suggested that the peripheral flow in malignant lymph nodes is in aberrant arterioles or veins with in the capsule, subcapsular area or surrounding connective tissue (5).

Previous studies suggested that unlike metastases, lymphomatous nodes tend to have mixed vascularity, while peripheral vascularity is relatively less common (16,30).

Analysis of spectral waveforms was useful and statistically significant in differentiating benign from malignant cervical lymphadenopathy. Metastatic nodes and lymphomatous nodes predominantly had high resistance pattern (cut off values $RI > 0.77$, $PI > 1.61$). RI was most specific for metastatic nodes while PI was most specific for lymphomatous nodes.

Different cut-off points for RI and PI were used in previous studies (4,16,31). The results of our study showed that there was a statistically significant difference between the mean values of RI and PI for benign and malignant nodes ($p < 0.05$ for RI and $p < 0.05$ for PI), which was comparable with previous studies (32,33). However, the other studies showed that benign and malignant lymph nodes cannot be distinguished solely on the basis of these Doppler indices (16,34,35).

In cases when color Doppler USG indicates the presence of malignant nodes, FNAC / biopsy is required to confirm the findings in an attempt to reach final diagnosis. Although color Doppler USG evaluation cannot replace histopathological procedure in knowing the status of cervical lymphadenopathy, it plays a definite role as an adjunct to the clinical evaluation of cervical lymphadenopathy and proves its value as an important investigation for differentiating between benign and malignant lymphadenopathy.

USG with power Doppler had sensitivity 74% and specificity of 96% for differentiating benign from malignant nodes (35).

The efficacy of USG (power Doppler USG plus gray-scale USG, 0.97 ± 0.005 ; gray-scale USG, 0.95 ± 0.004) for differentiate benign from malignant cervical lymph nodes and depict the internal architecture of the nodes was significantly greater than for CT (0.87 ± 0.018)(35).

As in every study, there were also *drawbacks* in our study. To start with, the sample size was small due to which exact distribution and morphology of the lymph nodes could not be studied. There was no uniformity in selection of the malignant nodes according to the stage of the disease. As all the patients have not undergone biopsy, the extracapsular spread could not be exactly evaluated. Moreover, tuberculosis infiltration of lymph nodes leads to destruction of the lymph node architecture in a manner similar to tumor infiltration, so these lymph nodes show similar USG and Doppler findings with malignant lymph nodes.

VI. Conclusion

To conclude, gray scale USG coupled with Doppler is a useful investigation in the evaluation of cervical adenopathy. USG is very useful as it is non-invasive, inexpensive, readily available and free of radiation. It can also be used as an imaging tool for the guided aspirations. Doppler indices are useful adjunct. USG with Doppler is helpful to differentiate benign from malignant causes of lymphadenopathy. However, USG lacks the ability of predicting the primary site of malignancy as compared to CT. USG and Color Doppler is particularly relevant in developing countries which have limited availability of CT & MRI scanners. USG & Color Doppler findings in addition to being radiation free are very useful and may avoid biopsy /FNAC.

References

- [1]. Ahuja AT, Ying M, Ho SY, Antonio G, Lee YP, King AD, et al. Ultrasound of malignant cervical lymph node. *Cancer Imaging* 2008;8:48-56.
- [2]. Ghafoori M, Azizian A, Pourrajabi Z, Vaseghi H. Sonographic Evaluation of Cervical Lymphadenopathy; Comparison of Metastatic and Reactive Lymph Nodes in Patients With Head and Neck Squamous Cell Carcinoma Using Gray Scale and Doppler Techniques. *Iran J Radiol* 2015;12: e11044.
- [3]. Benjamin J. Ludwig, Jimmy Wang, Rohini N. Nadgir, Naoko Saito, Ilse Castro-Aragon and Osamu Sakai. Imaging of Cervical Lymphadenopathy in Children and Young Adults. *Ajr* 2012;199:1105-1113.
- [4]. Brnic Z, Hebrang A. Usefulness of Doppler waveform analysis in differential diagnosis of cervical lymphadenopathy. *Eur Radiol* 2003;13:175-180.
- [5]. Ahuja AT, Ying M, Ho SSY, Metreweli C. Distribution of intranodal vessels in differentiating benign from metastatic neck nodes. *Clin Radiol* 2001;56:197-201.
- [6]. Van den Brekel MW, Castelijns JA, Stel HV, Golding RP, Meyer CJ, Snow GB. Modern imaging techniques and ultrasound-guided aspiration cytology for the assessment of neck node metastases: a prospective comparative study. *Eur Arch Otorhinolaryngol* 1993;250:11-17.
- [7]. Jenny K. Hoang, Jyotsna Vanka, Benjamin J. Ludwig, Christine M. Glastonbury. Evaluation of Cervical Lymph Nodes in Head and Neck Cancer With CT and MRI: Tips, Traps, and a Systematic Approach. *AJR* 2013;200:W17-W25.
- [8]. Van den Brekel MWM, Stel HV, Castelijns JA. Cervical lymph node metastasis: Assessment of radiologic criteria. *Radiology* 1990;177:379-84.
- [9]. Van den Brekel MWM, Castelijns JA, Snow G. Detection of lymph node metastases in the neck: radiologic criteria. *Radiology* 1994;192:617-618.
- [10]. Shah JP, Cendon RA, Farr HW, Strong EW. Carcinoma of the oral cavity: factors affecting treatment failure at the primary site and neck. *Am J Surg* 1976;132:504-507.
- [11]. Som PM, Curtin HD, Mancuso AA. Imaging based nodal classification for evaluation of neck metastatic adenopathy. *Am J Roentgenol* 2000;174:837-844.
- [12]. Dragoni F, Cartoni C, Pescarmona E, Chiarotti F, Puopolo M, Orsi E, et al. The role of high resolution pulsed and color Doppler ultrasound in the differential diagnosis of benign and malignant lymphadenopathy: results of multivariate analysis. *Cancer* 1999;85:2485-2490.
- [13]. Trotta BM, Pease CS, Rasamny JJ, Raghavan P, Mukherjee S. Oral cavity and oropharyngeal squamous cell cancer: key imaging findings for staging and treatment planning. *RadioGraphics* 2011;31:339-354.
- [14]. Nakamura T, Sumi M. Nodal imaging in the neck: recent advances in US, CT and MR imaging of metastatic nodes. *Eur Radiol* 2007;17:1235-1241.
- [15]. Vassallo P, Wernecke K, Roos N, Peters PE. Differentiation of benign from malignant superficial lymphadenopathy: the role of high resolution. *US Radiol* 1992; 183:215-220.
- [16]. Na DG, Lim HK, Byun HS, Kim HD, Ko YH, Baek JH. Differential diagnosis of cervical lymphadenopathies: usefulness of color Doppler sonography. *Am J Roentgenol* 1997;168:1311-1316.
- [17]. Solbiati L, Cioffi V, Ballarati E. Ultrasonography of neck. *Radiol Clin North Am* 1992;30:941-954.
- [18]. Som PM. Detection of metastasis in cervical lymph nodes: CT and MR criteria and differential diagnosis. *Am J Roentgenol* 1992;158:961-969.
- [19]. Ishii J, Hirokazu N, Yamane M, Hitoshi I, Yamashiro MT, Amagasa T, Kurabayashi T. Ultrasonography and computed tomography of extracapsular invasion in cervical lymph nodes of squamous cell carcinoma in the oral cavity. *J Med Ultrasonics* 2004; 31(2):74-79.
- [20]. Ahuja A, Ying M. An overview of neck node sonography. *Invest Radiol* 2002;37: 333-342.
- [21]. Rubaltelli L, Proto E, Salmaso R, Bortoletto P, Candiani F, Cagol P. Sonography of abnormal lymph nodes in vitro: correlation of sonographic and histologic findings. *Am J Roentgenol* 1990;155:1241-1244.
- [22]. Chang D-B, Yuan A, Yu C-J, Luh K-T, Kuo S-H, Yang P-C. Differentiation of benign and malignant cervical lymph nodes with color Doppler sonography. *Am J Roentgenol* 1994;162:965-968.
- [23]. Dolan PA. Tumor calcification following therapy. *Am J Roentgenol* 1963;89:166-74.
- [24]. Williams MP, Cherryman GR. Lymph node calcification in Lennert's lymphoma. *Br J Radiol* 1987;60:1131-1132.
- [25]. Wycoco D, Raval B. An unusual presentation of mediastinal Hodgkin's lymphoma on computed tomography. *J Comput Tomogram* 1983;7:187-188.
- [26]. Ahuja A, Ying M. Sonography of neck lymph nodes. Part II: Abnormal lymph nodes. *Clin Radiol* 2003;58:359-366.
- [27]. King AD, Tse GMK, Ahuja AT, Yuen EH, Vlantis AC, To EW, et al. Necrosis in metastatic neck nodes: diagnostic accuracy of CT, MR imaging, and US. *Radiology* 2004;230:720-726.
- [28]. Jeong HS, Baek CH, Son YI, Ki Chung M, Kyung Lee D, Young Choi J, et al. Use of integrated 18F-FDG PET/CT to improve the accuracy of initial cervical nodal evaluation in patients with head and neck squamous cell carcinoma. *Head Neck* 2007;29:203-210.
- [29]. Bruneton JN, Roux P, Caramella E, Demard F, Vallicioni J, Chauvel F. Ear, nose and throat cancer, ultrasound diagnosis of metastasis to cervical lymph nodes. *Radiology* 1984;162:771-773.
- [30]. Ahuja A, Ying M, Yuen YH, Metreweli C. Power Doppler sonography to differentiate tuberculous cervical lymphadenopathy from nasopharyngeal carcinoma. *AJNR* 2001;22:735-740.
- [31]. Steinkamp H-J, Mueffelmann M, Bock JC, Thiel T, Kenzel P, Felix R. Differential diagnosis of lymph node lesions: a semiquantitative approach with color Doppler ultrasound. *Br J Radiol* 1998;71:828-833.
- [32]. Shirakawa T, Miyamoto Y, Yamagishi J, Fukuda K, Tada S. Color/power Doppler sonographic differential diagnosis of superficial lymphadenopathy metastasis, malignant lymphoma, and benign process. *J Ultrasound Med* 2001;20:525-532.
- [33]. Ahuja A, Ying M, King W, Metreweli C. A practical approach to ultrasound of cervical lymph nodes. *J Laryngol Otol* 1997;111:245-256.
- [34]. Chang D-B, Yuan A, Yu C-J, Luh K-T, Kuo S-H, Yang P-C. Differentiation of benign and malignant cervical lymph nodes with color Doppler sonography. *Am J Roentgenol* 1994;162:965-968.
- [35]. Sumi M, Ohki M, Nakamura T. Comparison of sonography and CT for differentiating benign from malignant cervical lymph nodes in patients with squamous cell carcinoma of the head and neck. *Am J Roentgenol* 2001;176:1019-1024.

Table 1: An Imaging based nodal classification (adapted from Som P.M., Curtin H.D, Mancuso A.A.)¹¹ is now widely used for reporting of CT scan of neck.

Level	Definition of nodes
I	Above hyoid bone Below mylohyoid muscle Anterior to back of submandibular gland
IA	Between medial margins of anterior bellies of digastric muscles Previously classified as submental nodes
IB	Posterolateral to level IA nodes Previously classified as submandibular nodes
II	From Skull base to level of lower body of hyoid bone Posterior to back of submandibular gland Anterior to back of sternocleidomastoid muscle
IIA	Anterior, lateral, medial, or posterior to internal jugular vein Inseparable from internal jugular vein (if posterior to vein) Previously classified as upper internal jugular nodes
IIB	Posterior to internal jugular vein with fat plane separating nodes and vein Previously classified as upper spinal accessory nodes
III	From level of lower body of hyoid bone to level of lower cricoid cartilage arch Anterior to back of sternocleidomastoid muscle Previously known as mid jugular nodes
IV	From level of lower cricoid cartilage arch to level of clavicle Anterior to line connecting back of sternocleidomastoid muscle and posterolateral margin of anterior scalene muscle Lateral to carotid arteries Previously known as low jugular nodes
V	Posterior to back of sternocleidomastoid muscle from skull base to level of lower cricoid arch. From level of lower cricoid arch to level of clavicle as seen on each axial scan. Posterior to line connecting back of sternocleidomastoid muscle and posterolateral margin of anterior scalene muscle. Anterior to anterior edge of trapezius muscle
VA	From skull base to level of bottom of cricoid cartilage arch Posterior to back of sternocleidomastoid muscle Previously known as upper level V nodes
VB	From level of lower cricoid arch to level of clavicle as seen on each axial scan Posterior to line connecting back of sternocleidomastoid muscle and posterolateral margin of anterior scalene muscle Previously known as lower level V nodes
VI	Between carotid arteries from level of lower body of hyoid bone to level superior to top of manubrium Previously known as visceral nodes
VII	Between carotid arteries below level of top of manubrium Caudal to level of innominate vein Previously known as superior mediastinal nodes
Supraclavicular	At or caudal to level of clavicle as seen on each axial scan Above and medial to ribs
Retropharyngeal	Within 2 cm of skull base and medial to internal carotid arteries

Table 2: High resolution ultrasound findings

Features	Meta-static (n=66)	Lymphoma (n=27)	Level of Significance
Distribution			
Bilateral	21 (31.8%)	15 (55.6%)	p=0.669
Unilateral	45 (68.2%)	12 (44.4%)	
Size >10 mm (short axis)	45 (68.2%)	24 (88.9%)	p=0.209
Size (Mean±SD)	1.73±0.99	1.78±0.79	p=0.999
L/S ratio (Mean±SD)	1.86±0.73	2.01± 0.93	p=0.683
Shape			
Oval	21 (31.8%)	9 (33.3%)	p=0.276
Round	45 (68.2%)	18 (66.7%)	
Margins			
Blurred	24 (36.4%)	6 (22.2%)	p=0.549
Well defined	42 (63.6%)	21 (77.8%)	
Hilum			
Lost	48 (72.7%)	18 (66.7%)	p=0.980
Present	18 (27.3%)	9 (33.3%)	
Echotexture			
Hypoechoic	24 (36.4%)	18 (66.7%)	p=0.042
Heteroechoic	42 (63.6%)	9 (33.3%)	

Hyperechoic	0 (0%)	0 (0%)	
Calcification	3 (4.5%)	6 (22.0%)	p=0.139
Necrosis	51 (77.3%)	12 (44.4%)	p=0.037
Matting	33 (50.0%)	6 (22.2%)	p=0.414

n=no of patients, L/S=long axis/short axis.

Table 3: Color Doppler Findings

Features	Meta-static (n=22)	Lymphoma (n=9)	Level of Significance
Mean RI±SD	0.81±0.14	0.80±0.09	p=0.016
Mean PI±SD	2.44±1.21	2.30±1.03	p=0.010
Vascularity			
Absent	0 (0.0%)	3 (11.1%)	p=0.395
Peripheral	24 (36.4%)	0 (0%)	p=0.219
Mixed	21 (31.8%)	12 (44.4%)	p=0.173
Hilar	21 (31.8%)	12 (44.4%)	p=0.303

Table 4: Common sites of metastatic, lymphomatous and tuberculous nodes in the neck:¹²

Site	Commonly involved nodal groups
Metastases from oropharynx, hypopharynx, larynx carcinomas	Internal jugular chain
Metastases from oral cavity carcinomas	Submandibular Upper cervical
Metastases from infraclavicular carcinoma	Supraclavicular fossa Posterior triangle
Metastases from nasopharyngeal carcinoma	Upper cervical Posterior triangle
Metastases from papillary carcinoma of the thyroid	Internal jugular chain
Metastases from non-head and neck carcinoma	Supraclavicular fossa Posterior triangle
Non Hodgkin’s Lymphoma	Submandibular Upper cervical Posterior triangle
Tuberculosis	Supraclavicular fossa Posterior triangle

Legends

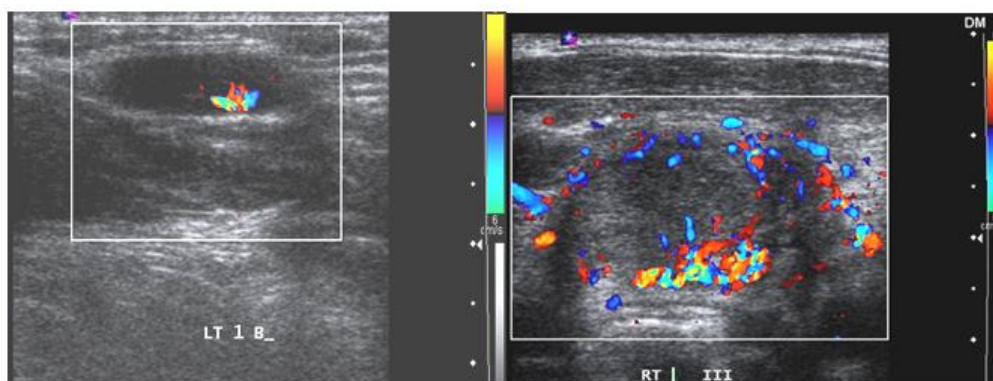
Fig. 1 A, B, C & D. Different patterns of vascularity on color doppler.

A-Hilar, B-Peripheral, C-Mixed, D-Avascular

Fig. 2A &B. 63 Yrs old male, FNAC proven metastatic CA. (A) Gray scale image shows a large (31.3x22.9 mm) matted, heterogeneous, ill defined level II A lymph nodal mass (arrow) with cystic necrosis. (B) Color Doppler shows peripheral vascularity.

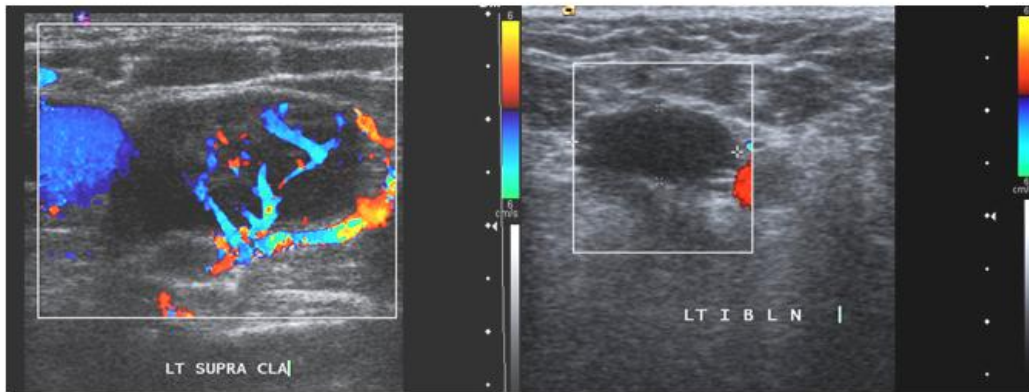
Fig. 3A, B &C. 51 Yrs old male patient with biopsy proven metastatic CA. (A) USG image showing heteroechoic, necrotic, matted right(RT) level IIA lymph nodes (arrow).(B&C) Color Doppler and Power Doppler show mixed vascularity.

Fig. 4. 75 Yrs old male patient with FNAC proven Hodgkin's lymphoma: USG image showing well defined hypoechoic lymph node with calcification (arrow) at level II A.

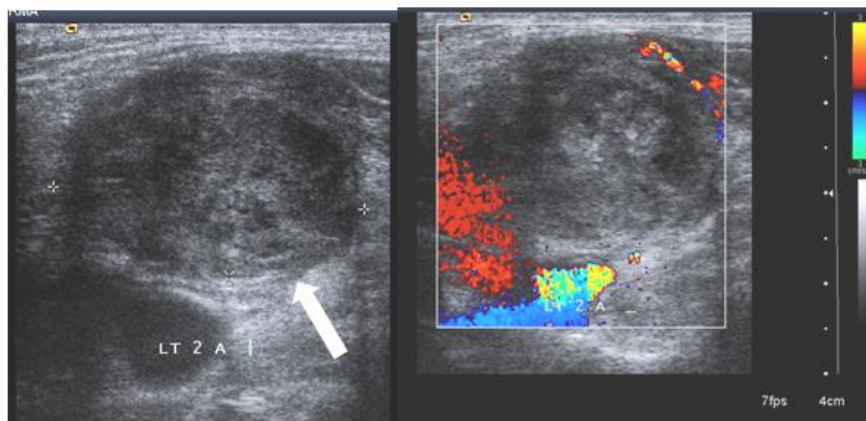


1A

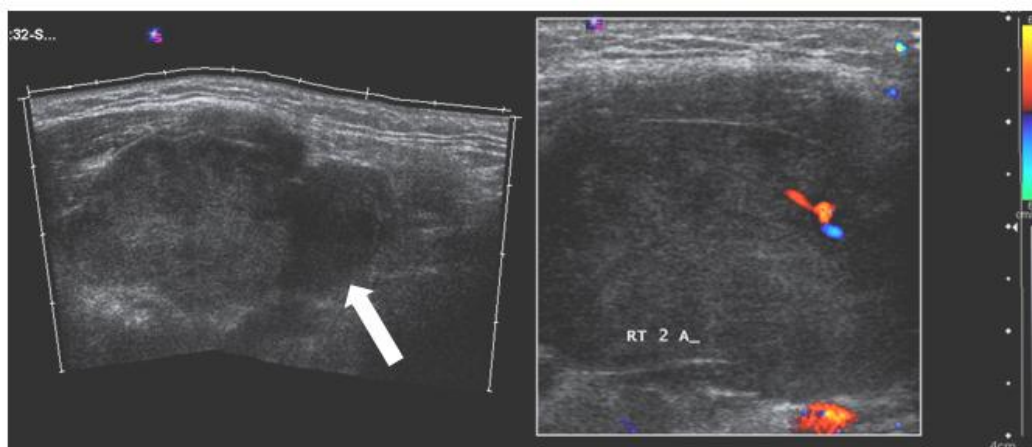
1B



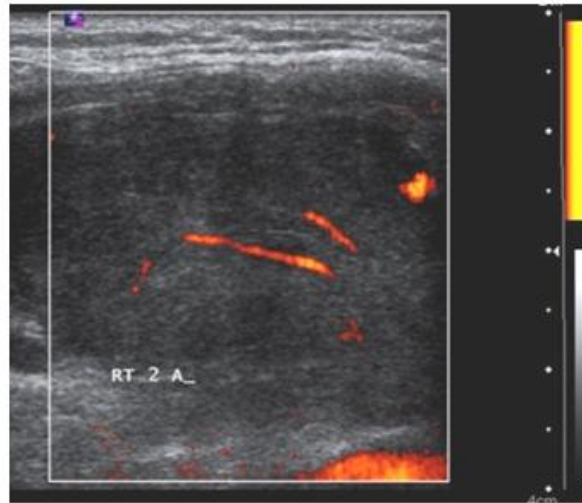
1C **1D**
FIG. 1 A, B, C & D: Different patterns of vascularity on color doppler.
 A-Hilar, B-Peripheral, C-Mixed, D-Avascular



2A **2B**
Fig 2: A & B : 63 Yrs old male, FNAC proven metastatic CA.
 A-Gray scale image shows a large (31.3x22.9 mm) matted, heterogeneous, ill defined level II A lymph nodal mass (arrow) with cystic necrosis.
 B-Color Doppler shows peripheral vascularity.

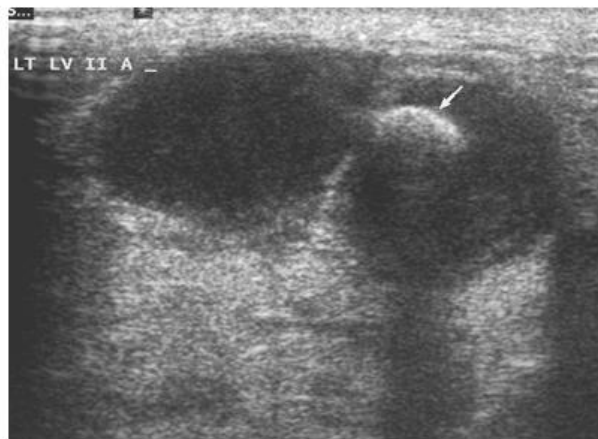


3A **3B**



3C

Fig. 3. A, B & C. 51 Yrs old male patient with biopsy proven metastatic CA. (A) USG image showing heteroechoic, necrotic, matted right(RT) level IIA lymph nodes (arrow). (B&C) Color Doppler and Power Doppler show mixed vascularity.



4

Fig. 4. 75 Yrs old male patient with FNAC proven Hodgkin's lymphoma. USG image showing well defined hypoechoic lymph node with calcification (arrow) at level II A.

Dr. Disha Mittal. “Evaluation Of high resolution Ultrasound With color Doppler findings In Malignant Cervical Lymphadenopathy.” IOSR Journal of Dental and Medical Sciences (IOSR-JDMS), vol. 18, no. 5, 2019, pp 07-15.